

# Physics with Single Photons plus Missing Energy Final States at DØ

**Edgar Carrera for the DØ Collaboration**

Florida State University, Tallahassee, FL 32306, USA

**Abstract.** Final state signatures of a single photon and missing transverse energy offer unique and powerful advantages in the search for new physics. This document presents the first observation of the  $Z\gamma \rightarrow \nu\bar{\nu}\gamma$  process at the Tevatron Collider at 5.1 standard deviations significance, as well as some of the strongest limits on anomalous trilinear  $ZZ\gamma$  and  $Z\gamma\gamma$  couplings to date. Additionally, we present the latest DØ results on a search for direct production of Kaluza Klein gravitons in association with single photons.

## 1. Introduction

In the standard model (SM), trilinear gauge boson electroweak interactions involving photons and  $Z$  bosons are forbidden at the leading-order level. Since next-to-leading order corrections to  $Z\gamma\gamma$  or  $ZZ\gamma$  vertices are small, an enhanced  $Z\gamma$  production rate, particularly at higher values of the photon transverse energy ( $E_T$ ), would indicate anomalous values of the trilinear gauge couplings (ATGC) and therefore presence of physics beyond the SM [1, 2]. These couplings can be parametrized as eight complex numbers of the form,  $h_i^V = h_{i0}^V/(1 + \hat{s}/\Lambda^2)^m$  [3], where  $i = 1, \dots, 4$  and  $V = Z, \gamma$ . Here, the subscript “0” indicates the low energy approximations of the couplings,  $\hat{s}$  is the square of the parton center-of-mass energy,  $\Lambda$  is the energy scale related to novel interactions responsible for new physics,  $m = 3$  for  $h_1^V$  and  $h_3^V$ , and  $m = 4$  for  $h_2^V$  and  $h_4^V$  [3]. The choice of the form factor, with the given values of  $m$ , guarantees the preservation of unitarity conditions at high energy. We study, using  $3.6 \text{ fb}^{-1}$  of data, the  $Z\gamma$  production where the  $Z$  boson decays to  $\nu\bar{\nu}$ . This final state, whose collider signature can be inferred by the presence of a single reconstructed photon and missing transverse energy ( $\cancel{E}_T$ ), is the most sensitive to ATGC, thanks to the large branching ratio (BR) of the  $Z$  boson to the invisible channel. This allows us to set limits on the size of the real parts of the ATGC.

The single photon signature and missing energy can also be used to search for the presence of large extra spatial dimension (LED) in our universe. In these scenarios [4], SM particles are bound to the ordinary 3-dimensional space, while the gravitational field exists as quantized towers of Kaluza-Klein (KK) modes (known as KK gravitons,  $G_{KK}$ ) in the extra space created by  $n$  large extra dimensions of size  $R$ . The large unexplained difference between the effective Planck mass scale in the 4-dimensional space-time ( $M_{Pl} \sim 10^{19} \text{ GeV}/c^2$ ) and the electroweak scale ( $\sim 10^3 \text{ GeV}/c^2$ ), can be solved since the fundamental Planck scale in the  $(4+n)$ -dimensional space-time ( $M_D$ ), which could be of the order of the electroweak scale, is concealed by the large size of the extra volume:  $M_{Pl}^2 = 8\pi M_D^{n+2} R^n$ . In this analysis we set limits to  $M_D$ , using  $2.7 \text{ fb}^{-1}$  of data, by studying the  $Z\gamma$ -analogous process  $q\bar{q} \rightarrow G_{KK}$  where the  $G_{KK}$  is not detected. These results constitute an update to Ref. [5].

## 2. Event Selection

The data used in both analyses are separated in two different datasets with different luminosity profiles, which result in different efficiencies and backgrounds. They were collected with the DØ detector [6], which consists of a central tracking system housed within a 2 T superconducting solenoid magnet, a preshower system, a liquid-argon calorimeter with fine-segmented electromagnetic (EM) and hadronic sections and a muon spectrometer with its own 1.8 T iron toroidal magnet. Events are required to pass trigger sets that demand at least one energy cluster in the EM section of the calorimeter with  $E_T > 20$  GeV. These trigger requirements are fully efficient for photons with  $E_T > 90$  GeV.

Photons are identified in the calorimeter as narrow clusters with at least 95% of their energy in the EM section. These clusters are required to be isolated in the calorimeter, *i.e.*, the isolation variable,  $\mathcal{I} = (E_{0.4}^{\text{tot}} - E_{0.2}^{\text{em}})/E_{0.2}^{\text{em}}$ , is required to be less than 0.07. In this equation,  $E_{0.4}^{\text{tot}}$  denotes the total energy deposited in the calorimeter in a cone of radius  $\mathcal{R} = \sqrt{(\Delta\eta)^2 + (\Delta\phi)^2} = 0.4$  [7] and  $E_{0.2}^{\text{em}}$  is the EM energy in a cone of radius  $\mathcal{R} = 0.2$ . The track isolation variable, defined as the scalar sum of the transverse momenta of all tracks that originate from the interaction vertex in an hollow cone of  $0.05 < \mathcal{R} < 0.4$  around the cluster, is required to be less than 2 GeV. The only EM clusters considered are the ones reconstructed within the central region of the detector ( $|\eta| < 1.1$ ) and consistent with the longitudinal and transverse shower shape profiles of a photon. Additionally, we require that there is no reconstructed track associated with the cluster nor a significant density of hits in the tracking system in agreement with that of a charged track. The EM cluster is required to have an associated energy cluster in the central preshower system (CPS).

We select the photon sample by requiring events with a photon candidate of  $E_T > 90$  GeV and  $\cancel{E}_T > 70$ , which effectively suppresses the multijet background. The  $\cancel{E}_T$  is computed from calorimeter cells and corrected from EM and jet energy scales. Jets with  $E_T > 15$  GeV are rejected in order to minimize large  $\cancel{E}_T$  due to jet energy mismeasurement. Events with muons, cosmic ray muons and energetic additional EM objects or tracks are rejected as well.

## 3. Analysis

In order to reduce the large background from cosmic ray muons and beam halo particles (together referred as non-collision background) that deposit energy in the calorimeter and mimic the signal signature, we require at least one interaction vertex consistent with the direction of the photon as given by the “pointing” algorithm. Assuming that EM showers are originated by photons, the EM pointing algorithm predicts the distance of closest approach to the  $z$  axis along the beam line and the  $z$  position of the interaction vertex in the event, independently of the tracker information and based solely on the calorimeter and the CPS. The remaining non-collision background and the backgrounds that arise from jet misidentification in  $W/Z$  events, are estimated by fitting the photon sample DCA distribution, as it is explained in detail in Ref. [5], to a linear sum of three DCA templates: a signal-like template, a non-collision template and a misidentified jets template. The procedure estimates the fractional contribution of these components.

The number of background events from the electroweak process  $W \rightarrow e\nu$ , where the electron is misidentified as a photon, is estimated by selecting an electron sample with the same kinematical requirements as the photon sample, and scaling the final number of events by the measured rate of electron-photon misidentification. The  $Z\gamma \rightarrow \nu\bar{\nu}\gamma$  (for the LED analysis only) and the  $W\gamma$  background, where the  $W$  boson decays leptonically and the lepton is not detected, are estimated using samples of Monte Carlo (MC) events, which are generated using PYTHIA [8], put through a GEANT-based [9] DØ detector simulation program and reconstructed with the same software as used for data. Differences between data and simulation are corrected by applying scale factors. A summary of backgrounds, for both analyses, is shown in Table 1.

The signal process  $\gamma G_{KK}$  is generated [10] using PYTHIA for number of extra dimensions

**Table 1.** Summary of background estimates, and the number of observed and SM predicted events. The numbers represent a combination of two separate data sets with different profiles of the instantaneous luminosity.

Process	ATGC Analysis $3.6 \text{ fb}^{-1}$	LED Analysis $2.7 \text{ fb}^{-1}$
$Z\gamma \rightarrow \nu\bar{\nu}\gamma$	–	$29.5 \pm 2.5$
$W \rightarrow e\nu$	$9.67 \pm 0.56$	$8.5 \pm 1.7$
non-collision	$5.33 \pm 1.95$	$6.6 \pm 2.3$
$W/Z + \text{jet}$	$1.37 \pm 0.95$	$3.1 \pm 1.5$
$W\gamma$	$0.90 \pm 0.14$	$2.22 \pm 0.3$
Total background	$17.3 \pm 2.38$	$49.9 \pm 4.1$
$N_{\nu\bar{\nu}\gamma}^{\text{SM}}$	$33.7 \pm 3.4$	–
$N_{\text{obs}}$	51	51

ranging from 2 to 8 and for a  $M_D$  value of  $1.5 \text{ GeV}/c^2$ . A total luminosity-averaged efficiency of about 43% is estimated for central photons of  $E_T > 90 \text{ GeV}$ . No NLO order K-factors are applied to the LED signal. The number of observed events ( $N_{\text{obs}}$ ) can be seen in Table 1.

In order to estimate the acceptance of  $Z\gamma \rightarrow \nu\bar{\nu}\gamma$  events for photons of  $E_T > 90 \text{ GeV}$ , we use events from MC samples produced with a leading-order (LO)  $Z\gamma$  generator [11] that are passed through a parametrized simulation of the DØ detector. The expected number of events ( $N_{\nu\bar{\nu}\gamma}^{\text{SM}}$ ) according to this simulation and the number of observed events are shown in Table 1. The MC samples for the ATGC signal are produced with the LO  $Z\gamma$  generator with values of  $h_{30}^V$  and  $h_{40}^V$  that differ from zero and for the form-factor scale  $\Lambda = 1.5 \text{ TeV}$ .

Next-to-leading order (NLO) QCD effects are predicted to be small for our event selection, and we assign 7% uncertainty to SM process cross sections due to them. Other sources of systematic uncertainty include uncertainty due to photon identification (5%), choice of parton distribution functions (7%) and uncertainty in the total integrated luminosity (6.1%).

#### 4. Results and Conclusions

The number of single photon candidate events are in agreement with the number of background events, therefore we proceed to set limits. In the case of LED analysis, we employ the modified frequentist approach [12, 13], using the binned photon  $E_T$  distribution, to set limits for  $M_D$  (Fig. 1) at the 95% confidence level (C.L.):  $M_D > 970, 899, 867, 848, 831, 834$  and  $804 \text{ GeV}/c^2$  for  $n = 2, 3, 4, 5, 6, 7$  and 8 extra dimensions.

The  $Z\gamma$  cross section multiplied by the BR of the invisible channel is measured to be  $32 \pm 9(\text{stat.} + \text{syst.}) \pm 2(\text{lumi.}) \text{ fb}$ , which is in good agreement with the SM NLO prediction of  $39 \pm 4 \text{ fb}$  [11]. The statistical significance of the measured cross section corresponds to 5.1 standard deviations (s.d.). Thus, this is the first observation of the  $Z\gamma \rightarrow \nu\bar{\nu}\gamma$  process at the Tevatron. Since the SM production and observed production agree, we set limits on ATGC at the 95% C.L. using a binned likelihood method, which compares, bin by bin, the photon  $E_T$  spectrum in data with the corresponding distribution from SM background and (“anomalous”)  $Z\gamma$  signal. The comparison is performed for each pair of couplings in a two dimensional grid involving  $h_{30}^V$  and  $h_{40}^V$ . Poisson distributions are assumed for data and ATGC signal, while uncertainties for the background, all systematic uncertainties and luminosity are assumed to be Gaussian. To calculate one-dimensional limits we set the additional anomalous coupling to zero. The one-dimensional limits in the neutrino channel are:  $|h_{30}^\gamma| < 0.036$ ,  $|h_{40}^\gamma| < 0.0019$  and  $|h_{30}^Z| < 0.035$ ,  $|h_{40}^Z| < 0.0019$ .

We combine the results in the invisible decay channel of the  $Z$  boson with the  $Z\gamma \rightarrow \ell\ell\gamma$  ( $\ell = e, \mu$ ) channels [16], which were studied in detail in [17] for  $1 \text{ fb}^{-1}$  of data. The one-

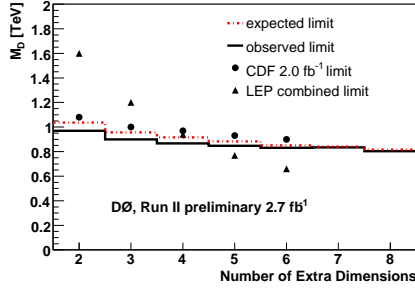


**Figure 1.** The expected and observed lower limits on  $M_D$  for LED in the  $\gamma + \cancel{E}_T$  final state. CDF limits with  $2 \text{ fb}^{-1}$  of data (single photon channel) [14], and the LEP combined limits [15] are also shown.

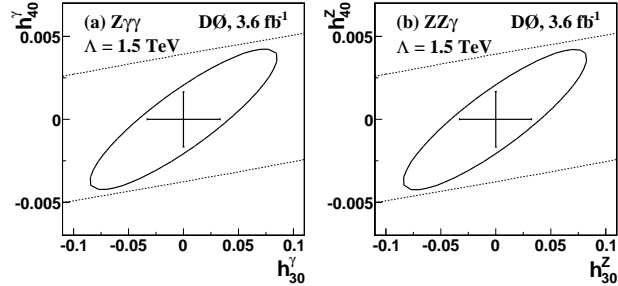


**Figure 2.** Two-dimensional bounds (ellipses) at 95% C.L. on CP-conserving (a)  $Z\gamma\gamma$  and (b)  $ZZ\gamma$  couplings. The crosses represent the one-dimensional bounds at the 95% C.L. setting all other couplings to zero. The dashed lines indicate the unitarity limits for  $\Lambda = 1.5 \text{ TeV}$ .

dimensional limits for the combination of the three channels are:  $|h_{30}^\gamma| < 0.033$ ,  $|h_{40}^\gamma| < 0.0017$  and  $|h_{30}^Z| < 0.033$ ,  $|h_{40}^Z| < 0.0017$ . We can assert that the limits on  $h_{30}^Z$ ,  $h_{40}^Z$ , and  $h_{40}^\gamma$  are the most restrictive to date. One and two-dimensional limits can be appreciated in Fig. 2

To summarize, we tested the strength of the electroweak force and searched for the presence of LED in our universe via single photon plus missing energy final states finding no hints of new physics. We observed, for the first time at the Tevatron, the  $Z\gamma \rightarrow \nu\bar{\nu}\gamma$  process at a statistical significance of 5.1 s.d. and set limits on the ATGC, some of which are the most restrictive to date.

## Acknowledgments

The author wishes to thank the staffs at Fermilab and collaborating institutions, principally Alexey Ferapontov, Yuri Gershtein and Yurii Maravin.

## References

- [1] Gounaris G J, Layssac J and Renard F M 2003 *Phys. Rev.* **D67** 013012 (*Preprint hep-ph/0211327*)
- [2] Choudhury D, Dutta S, Rakshit S and Rindani S 2001 *Int. J. Mod. Phys.* **A16** 4891–4910 (*Preprint hep-ph/0011205*)
- [3] Baur U and Berger E L 1993 *Phys. Rev. D* **47** 4889–4904
- [4] Arkani-Hamed N, Dimopoulos S and Dvali G R 1998 *Phys. Lett.* **B429** 263–272 (*Preprint hep-ph/9803315*)
- [5] Abazov V M *et al.* (D0) 2008 *Phys. Rev. Lett.* **101** 011601 (*Preprint 0803.2137*)
- [6] Abazov V M *et al.* (D0) 2006 *Nucl. Instrum. Meth.* **A565** 463–537 (*Preprint physics/0507191*)
- [7] The pseudo-rapidity  $\eta$  is defined as  $\eta = -\ln[\tan(\theta/2)]$ , where  $\theta$  is the polar angle measured with respect to the proton beam direction.  $\phi$  is the azimuthal angle.
- [8] Sjostrand T *et al.* 2001 *Comput. Phys. Commun.* **135** 238–259 (*Preprint hep-ph/0010017*)
- [9] Brun R and Carminati F CERN Program Library Long Writeup Report No. W5013, 1994
- [10] Mrenna S 2007 private communication
- [11] Baur U, Han T and Ohnemus J 1998 *Phys. Rev. D* **57** 2823–2836
- [12] Fisher W *Systematics and Limit Calculations* FERMILAB-TM-2386-E, 2007
- [13] Junk T 1999 *Nucl. Inst. Meth.* **A434** 435–443
- [14] Aaltonen T *et al.* (CDF) 2008 *Phys. Rev. Lett.* **101** 181602 (*Preprint 0807.3132*)
- [15] LEP Exotica Working Group. Combination of LEP Results on Direct Searches for Large Extra Dimensions: [http://lepexotica.web.cern.ch/LEPEXOTICA/notes/2004-03/ed\\_note\\_final.ps.gz](http://lepexotica.web.cern.ch/LEPEXOTICA/notes/2004-03/ed_note_final.ps.gz)
- [16] MC samples for these channels were regenerated with  $\Lambda = 1.5 \text{ TeV}$
- [17] Abazov V *et al.* 2007 *Phys. Lett. B* **653** 378–386